Control of Internal Moisture Transfer Direction and Lateral Moisturization to Mitigate Drying Defects in Large-Cross-Section Timber

Bat-Uchral Batjargal,[a,b] Taekyeong Lee,[c] Chang-Jin Lee,[d] Jung-Kwon Oh ,[a,c] and Hwanmyeong Yeo ,[a,c,*]

* *Corresponding author: hyeo@snu.ac.kr*

DOI: 10.15376/biores.20.2.4761-4775

GRAPHICAL ABSTRACT

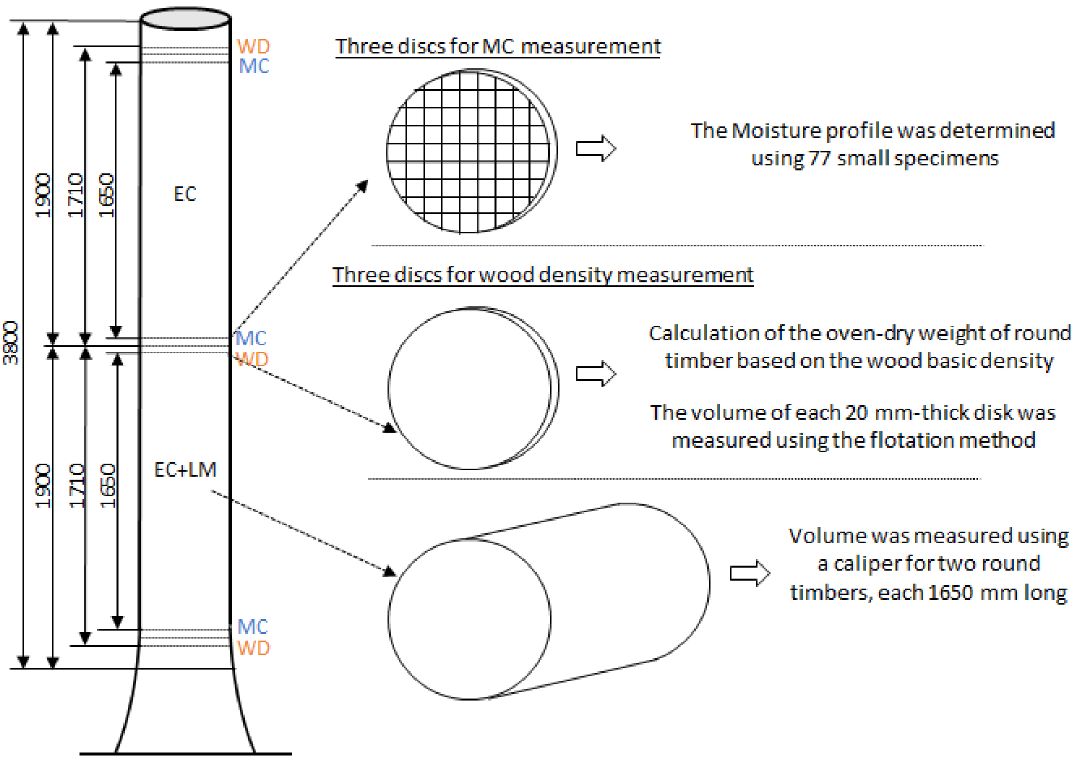

Control of Internal Moisture Transfer Direction and Lateral Moisturization to Mitigate Drying Defects in Large-Cross-Section Timber

Bat-Uchral Batjargal,[a,b] Taekyeong Lee,[c] Chang-Jin Lee,[d] Jung-Kwon Oh ,[a,c] and Hwanmyeong Yeo ,[a,c,*]

The drying process of large-cross-section timber is a critical challenge in the timber industry, as it is prone to moisture gradients and drying defects, such as surface checks and cracks, which negatively affect the wood's quality and structural integrity. Therefore, effective methods to control moisture movement during drying are essential for improving timber utilization and preserving its sustainability. This study investigated the effect of surface moisturization and internal moisture control in minimizing drying defects in large-cross-section Korean Red Pine (*Pinus densiflora*). The experimental setup involved applying cross-sectional sealing and steaming pre-treatment to regulate internal moisture transfer, with real-time monitoring of weight changes and moisture content at various positions within the timber using load cells and hygrometers. The results showed that lateral moisturization effectively mitigated drying defects by reducing the rate of moisture loss from the ends. The total drying time was 835.4 hours (approximately 35 days), and surface moisturization proved to be a critical factor in reducing surface checks and enhancing wood quality. This approach provides a promising strategy for improving drying efficiency and reducing defects, ultimately benefiting the timber industry by promoting more sustainable wood drying practices.

DOI: 10.15376/biores.20.2.4761-4775

Keywords: Kiln drying; Drying stress; Surface check; Surface moisturization; Large-cross section timber

Contact information: a: Department of Agriculture, Forestry and Bioresources, Seoul National University, Seoul, Republic of Korea; b: Training and Research Institute of Forestry and Wood Industry, Mongolian University of Science Technology, Ulaanbaatar, Mongolia; c: Research Institute of Agriculture and Life Sciences, Seoul National University, Seoul, Republic of Korea; d: Department of Wood Science and Technology, Jeonbuk National University, Jeonju, Republic of Korea;
** Corresponding author: hyeo@snu.ac.kr*

INTRODUCTION

Wood is essential in construction, furniture production, and various other industries. Its hygroscopic nature allows it to absorb and release moisture from the surrounding environment, making its quality highly dependent on the pre-treatment and drying processes (Srisuchart *et al.* 2023; Kim *et al.* 2020). The preservation and restoration of wooden cultural heritage sites, such as palaces and temples, often require large-cross-sectional timber to serve for structural elements, such as columns and beams (Han *et al.* 2019a,b; Lee 2020; Jung *et al.* 2022; Lee and Lee 2023). However, uneven drying often results in a significant internal moisture gradient, leading to drying stresses that cause structural defects such as cracks. Furthermore, it increases the likelihood of over-drying or under-drying, both of which can negatively impact the wood's structural integrity, durability, and sustainability for construction (Green *et al.* 1999; Skaar 1988; Redman *et al.* 2016; Kim *et al.* 2017).

Drying stress is closely related to internal factors, such as wood components, species, and moisture content, as well as external factors, such as drying temperature and relative humidity (Keey *et al*. 2000). Cracks often develop in areas with significant differences in shrinkage during drying, including the interfaces between heartwood and sapwood or the transition zones between earlywood and latewood (Oltean *et al*. 2007).

Recent studies have emphasized the importance of understanding and controlling internal moisture dynamics during drying (Penvern *et al*. 2020). Uwizeyimana *et al.* (2020) demonstrated that variables such as temperature and humidity significantly influence moisture content measurements and highlighted the ability of resistance sensors to track moisture movement within wood accurately. Additionally, lateral moisturization and moisture control techniques have been proven effective in uniformly regulating moisture loss, thereby reducing the likelihood of defects during drying (Elustondo *et al.,* 2023). Botter-Kuisch *et al*. (2020) measured the changes in wood weight during drying and placed temperature and humidity sensors at various depths within the wood. Their findings emphasized that effectively managing moisture gradients can control shrinkage and reduce internal stress. Furthermore, pretreatment methods such as steam treatment have been shown to delay initial moisture loss, promote balanced drying, and reduce the risk of defects (Yin and Liu 2021; Lee and Lee 2023). Techniques such as cross-sectional coating have proven effective in reducing surface checks, thereby preserving the structural integrity of timber (Fu *et al.* 2023).

Pretreatment techniques, such as pre-steaming, have been demonstrated to positively influence the drying characteristics of red pine timber (Lee and Lee 2023). Pre-steaming delays initial moisture loss, promoting a more uniform drying process and reducing the risk of defects associated with uneven internal moisture distribution(Li *et al.* 2019).

In the early stages of drying, drying stresses are generally minimal and do not compromise the structural integrity of the wood. However, as the moisture content (MC) decreased below the fiber saturation point, the drying stress increased progressively. Once these stresses exceed the tensile strength of the wood in the tangential direction, cracks and other drying defects may occur (Fu *et al.* 2016).

Moisture gradients within the timber are the primary cause of internal stress during drying, often leading to structural defects such as checking (Park *et al*. 2020). These stresses arise from differential drying rates between the outer and inner wood layers. The faster drying of the outer layers induces shrinkage, whereas the inner layers with a higher moisture content resist this shrinkage. This imbalance results in internal stresses that can cause splitting and checking, particularly during the initial drying stages when the MC falls below the fiber saturation point. Several factors typically influence checking, including the moisture content disparity between heartwood and sapwood, specimen thickness, and differences in tangential and radial shrinkage (Larsen and Ormarsson 2014; Hill *et al.* 2013).

This study employed a silica-gel-based blanket cover as an innovative, reusable, and sustainable solution for managing the lateral moisture content during the drying process of large-cross-section timber. No prior studies have utilized this specific silica-gel-based method for surface moisturization in timber drying. By optimizing internal moisture transfer and effectively reducing drying-induced stresses, this method significantly reduces the risk of cracks. Building on this approach, this study aimed to establish a controlled drying process for large-cross-sectional Korean red pine (*Pinus densiflora*) round timber. These techniques are designed to minimize moisture gradients, enhance wood quality, and promote technological advancements in the timber industry.

EXPERIMENTAL

Materials

The experiment utilized a single round of red pine timber with a diameter of 450 mm and length of 3800 mm. The specimens were prepared by removing 190 mm from each end of the timber. The remaining portion was divided into two sections measuring 1650 mm long. The average wood density of each specimen was 0.41 g/cm³. The average initial moisture content of the red pine timber before cutting into specimens was 94% (Fig. 1). Additionally, for the end-coating treatment, urethane waterproof paint (New Waterthane, Samhwa, Republic of Korea) was used, and for surface moisturization, a silica-gel-based blanket cover was created and applied.

Methods

Sample preparation

To analyze moisture content (MC) and wood density (WD) distributions, six disk-shaped specimens (20 mm thick) were extracted from three specific locations along the timber's length: both ends and the middle section (approximately 1900 mm from one end). Three disks from each location were used for MC and WD measurements. The preparation and sampling processes are illustrated in Fig. 1. The disk specimens designated for the MC measurements were further subdivided into 77 small test pieces for a detailed analysis of the internal MC distribution. The oven-drying method was used to ensure the accurate measurement of MC in these test pieces.

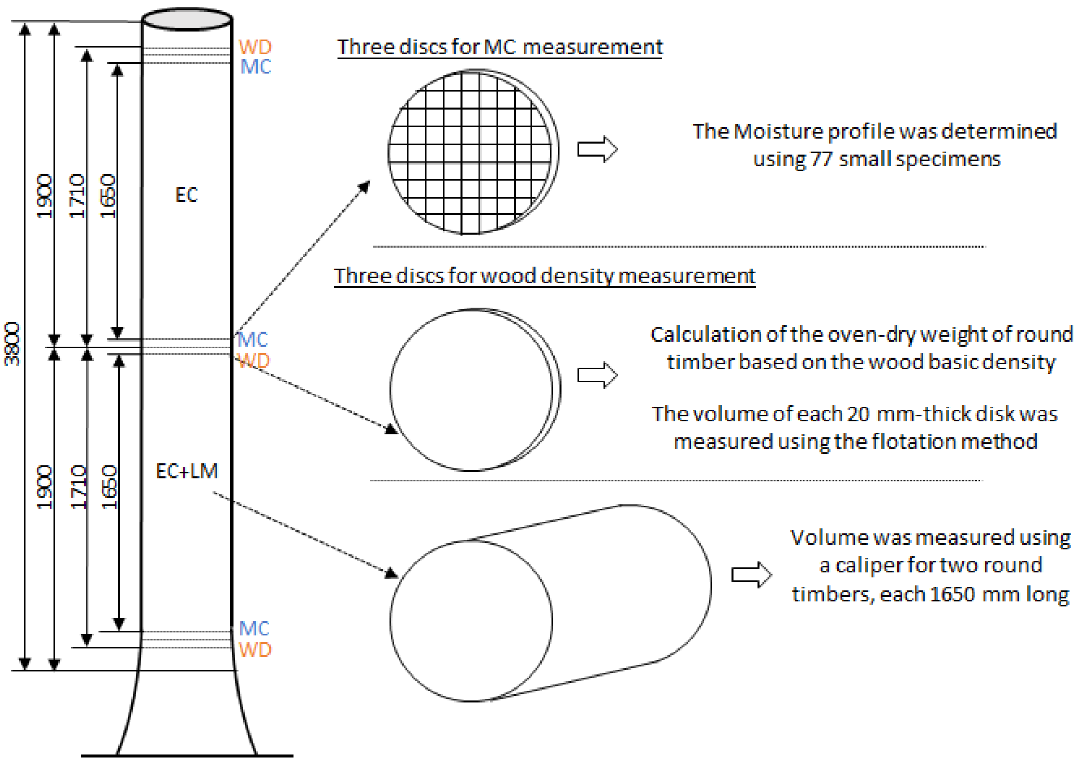

Fig. 1. Illustration of the experimental procedures. EC: End coating, EC+LM: End Coating + Lateral Moisturization, WD: Specimen for measuring wood basic density; MC: Specimen for measuring moisture content

End Coating and Lateral Moisturization Pre-treatment

This study implemented two pre-treatment methods:

1. End Coating (EC): The ends of the timber were coated with urethane waterproof paint to minimize moisture loss along the grain direction (Fig. 2 (a)). During the drying process, the lateral surface of the timber was exposed to outside air. (Batjargal *et al.* 2023).

2. End Coating with Lateral Moisturization (EC+LM): This treatment was based on the EC method. Once the timber MC reached approximately 50%, the critical point at which internal stresses began to develop, the lateral surface was wrapped with a silica-gel-based blanket cover. The purpose of this blanket was to control and regulate the moisture, preventing rapid drying and reducing internal stresses.

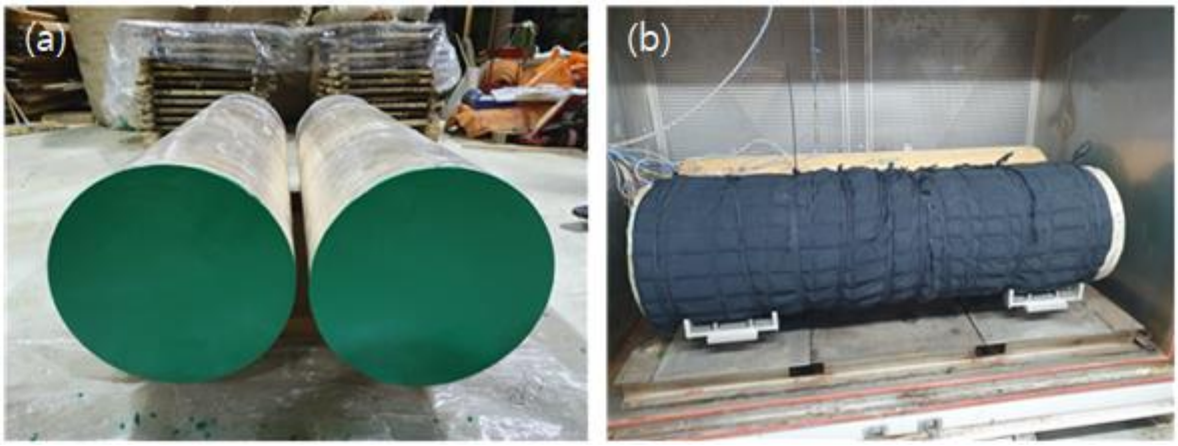

Fig. 2. Pretreatment for kiln drying: ends coated with urethane waterproof paint (a), applied silica gel cover (b)

Pre-steaming Treatment and Kiln Drying Schedule

Precise drying conditions were implemented to achieve a uniform moisture distribution across the timber cross-section. These conditions include careful temperature control, relative humidity (RH), and air flow velocity. A minimum air velocity of 2 m/s was maintained to prevent the formation of stagnant damp air zones around the timber, ensuring consistent drying across the surface. This air velocity was selected based on the capabilities of the kiln drying system used in the experiment, which was designed to maintain a minimum airflow of 2 m/s.

Table 1. Kiln Drying Schedule for Large-Cross-Section Timber

Step	Time (hours)	DBT. (℃)	WDBT diff. (℃)	WBT. (℃)	RH (%)	EMC (%)	MC (%)	Pre-treatment
0	126.4	70	0.5	69.5	99	22.0	green	Steaming
1	157.4	75	1.5	73.5	94	18.0	~70	EC
2	93.1	80	2.0	78.0	92	16.3	70~55	EC
3	69.0	80	5.5	74.5	79	11.3	55~40	EC+LM
4	51.5	90	8.5	81.5	71	8.6	40~30	EC+LM
5	71.9	80	1.5	78.5	90	15.3	30~25	EC+LM
6	245.0	80	5.5	74.5	79	11.3	~15	EC+LM

Note: DBT: Dry bulb temperature; WBT: Wet bulb temperature; WDBT diffusion, wet and dry bulb temperature difference; EMC: Equilibrium moisture content; RH: Relative Humidity; EC: End coating; EC + LM: End Coating with Lateral Moisturization; Includes 21-h cooling after drying.

The pre-steaming process was conducted at 70 °C and 99% RH for 120 h. Following the pre-steaming phase, the timber was subjected to a controlled drying schedule with a carefully managed temperature differential between the dry- and wet-bulb readings. The detailed drying schedule is presented in Table 1. The drying process was conducted using a kiln dryer (HB-503LF-0, Hanbeak, Republic of Korea) that offered precise environmental control to optimize the drying conditions.

Moisture Content and Wood Density Measurements

The average MC of the timber was determined using its basic density and initial weight, as outlined by Siau (1995). The average moisture content refers to the overall moisture content calculated by averaging the moisture measurements taken at multiple points along the timber. The wood density was calculated using Eq. (1), whereas the oven-dry weight of the timber was derived using Eq. (2). Subsequently, moisture loss over time was assessed using Eq. (3), which incorporates the oven-dry weight and measures the weights recorded during drying. In this section, the specific moisture content was obtained at different depths (20 mm, 80 mm) and positions (*e.g.*, 50 mm, 412 mm, and 825 mm from the end) within the timber, which provides insight into the moisture distribution and gradient across the specimen.

Weight measurements were conducted using a load cell (ZBCDS-500LH, CAS, Korea) and an electronic balance (AD-310A, A&D Korea), with data collected at 10-minute intervals. This continuous monitoring facilitated the real-time observation of the average moisture loss and enabled the determination of the MC gradient across the timber (Fig. 2 (b)).

$$\boldsymbol{\rho}_{(\mathbf{disk})} = \frac{\boldsymbol{W}_{\mathbf{od\ (disk)}}}{\boldsymbol{V}_{\mathbf{(disk)}}} \tag{1}$$

$$W_{\mathrm{od\ (timber)}} = V_{\mathrm{(timber)}} \times \rho_{\mathrm{(disk)}} \tag{2}$$

$$\mathrm{MC}_{\mathrm{(timber)}} = \frac{W_{\mathrm{g\ (timber)}} - W_{\mathrm{od\ (timber)}}}{W_{\mathrm{od}}\ \mathrm{(timber)}} \times 100\% \tag{3}$$

where: $\rho_{\mathrm{(disk)}}$ is the wood density of the cross-sectional disk (kg/m^3), $W_{\mathrm{od\ (disk)}}$ is the oven-dry weight of the disk (kg), $V_{\mathrm{(disk)}}$ is the volume of the disk specimen (m^3), $W_{\mathrm{od\ (timber)}}$ is the estimated oven-dry weight of the 1650 mm long timber (kg), $V_{\mathrm{(timber)}}$ is the volume of the 1650 mm long timber (m^3), $\mathrm{MC}_{\mathrm{(timber)}}$ is the MC of the 1650 mm long timber (%), and $W_{\mathrm{g\ (timber)}}$ is the actual weight of the 1650 mm long timber (kg).

Measurement Method and Procedure for Timber Volume

The timber volume was calculated based on the circumference and cross-sectional dimensions. Circumference measurements were obtained using diameter tape at five equidistant locations along the timber length. In addition, the cross-sectional width and length were measured at four locations per section. The average value of these measurements was used to calculate the overall timber volume.

Real-Time Measurement of Moisture Content Using Embedded Sensors

To monitor the MC and internal conditions during drying, temperature and humidity sensors were embedded within the timber at strategic locations (50 mm, 412 mm, and 825 mm from the end), as shown in Fig. 3 The sensor locations were chosen based on the assumption that moisture removal during drying occurs symmetrically. These specific measurements help track the moisture content at distinct locations, providing detailed insights into moisture gradients within the timber. The temperature and relative humidity at 10-minute intervals using a temperature and humidity logger

(LogE8 THE, Elitech Technology, USA) allowing real-time monitoring of both average and specific moisture content during the drying process.

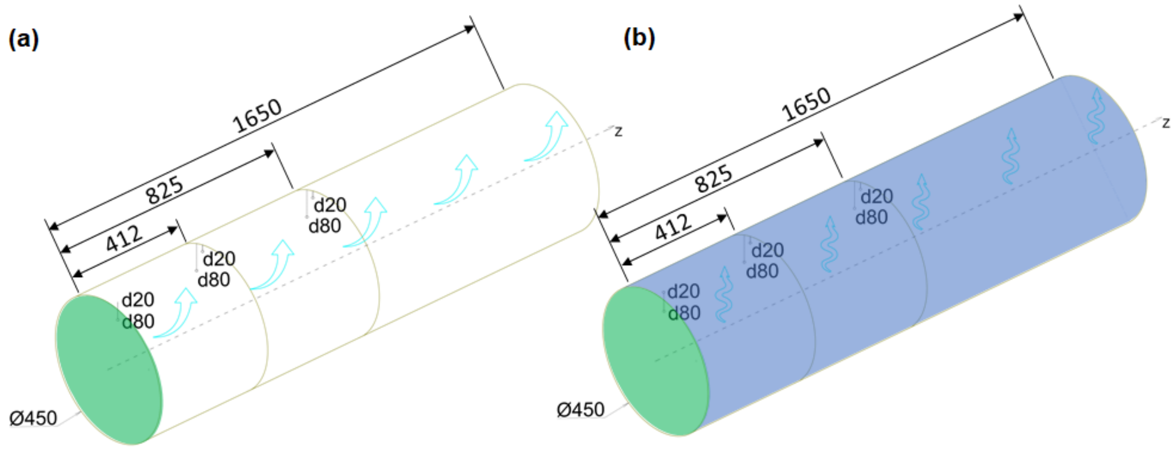

Fig. 3. A schematic diagram showing the location of inserted temperature and humidity sensors in the timbers and the pretreatment, (a) End Coating, (b) End Coating + Lateral Moisturization

The collected data were applied to the Hailwood-Horrobin model (Simpson, 1973) to calculate the equilibrium MC of the timber (Eq. 4). This real-time monitoring approach allowed the precise control of the drying process, ensuring minimal defects and enhanced product quality.

$$\mathrm{EMC} = \frac{\mathrm{RH}}{\mathrm{A+B{\cdot}RH-C{\cdot}RH^2}} \tag{4}$$

$$\mathrm{A} = \frac{\mathrm{W}}{0.018} \cdot \left[\frac{1}{\mathrm{K_2{\cdot}(K_1+1)}}\right]$$

$$\mathrm{B} = \frac{\mathrm{W}}{1.8} \cdot \left[\frac{\mathrm{K_1-1}}{\mathrm{K_1+1}}\right]$$

$$\mathrm{C} = \frac{\mathrm{W{\cdot}K_1{\cdot}K_2}}{180{\cdot}\,(\mathrm{K_1+1})}$$

$$\mathrm{W} = 0.2234{+}0.0007 \cdot \mathrm{T}{-}0.000019 \cdot \mathrm{T}^2$$

$$\mathrm{K_1} = 4.73{+}0.048 \cdot \mathrm{T}{-}0.0005 \cdot \mathrm{T}^2$$

$$\mathrm{K_2} = 0.706{+}0.0017 \cdot \mathrm{T}{-}0.000006 \cdot \mathrm{T}^2$$

where EMC is the Equilibrium Moisture Content (%), and RH is the Relative Humidity inside the wood (%). The parameters W, K_1, and K_2 are coefficients developed by the Hailwood-Horrobin adsorption model, and T is the temperature (°C).

Shrinkage and Surface Check Measurement Post-Drying

The shrinkage measurements were performed before and after drying. Using circumference-measuring tape, measurements were taken at five predetermined positions along the timber length (Fig. 3). The measurement of surface checks wider than 1 mm was performed because, during the post-drying process, smaller checks (less than 1 mm) are typically eliminated through processes such as planing. Therefore, only surface checks larger than 1 mm were considered in this study.

Final Moisture Content Distribution

After drying, the final MC distribution was analyzed by comparing the MC values of the disc samples collected at positions corresponding to the embedded sensor locations (50 mm, 412 mm, and 825 mm from the end). The oven-drying method was used to determine the final MC, allowing a direct comparison with real-time sensor data.

This comprehensive methodology provides a detailed understanding of the MC distribution, shrinkage behavior, and drying defects, which are critical for optimizing the drying processes in large-cross-section timbers.

RESULTS AND DISCUSSION

Initial Moisture Content Distribution

Initial Moisture Content (IMC) measurements revealed significant variations across the specimens, with the highest values observed in the outer layers (150%) and the lowest values in the core (30%). These results are consistent with the typical moisture distribution patterns in timber, where the outer layers generally retain more moisture than the core (Fig.4).

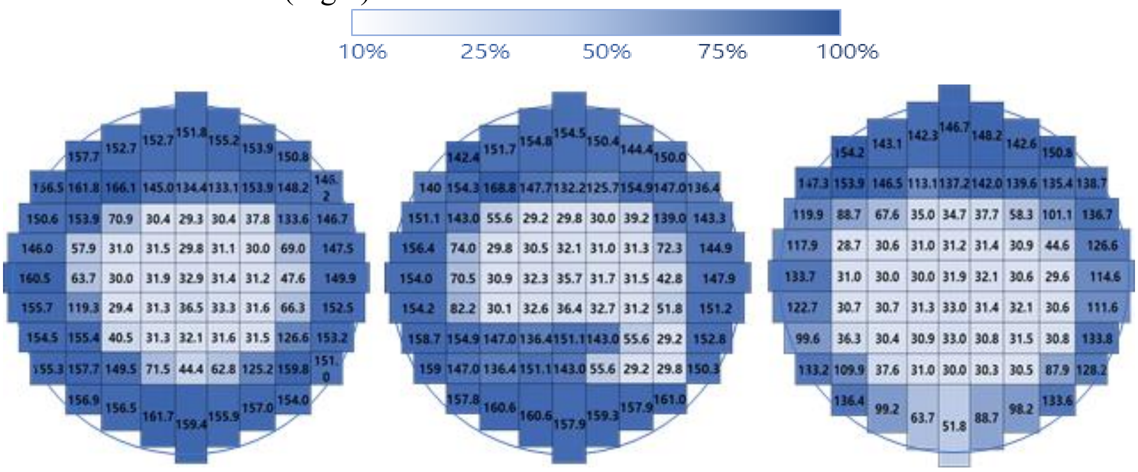

Fig. 4. IMC profile in wood disk taken at intervals of (a) 190 mm, (b) 1900 mm, (c) 3570 mm from the log butt

Wood Density and Moisture Content by Longitudinal Position

The three disk-shaped specimens were volumized using the displacement method and oven-dried to determine the dry weight for the wood density calculations. The results of wood density (WD) and moisture content (MC) at different locations along the length of the oversized logs are presented in Fig 5. The variation in wood density was smaller than that of MC along the longitudinal direction. This observation aligns with previous studies that reported similar trends in wood density variations (Simpson 1991; Kollmann and Côté 1968). The IMC was calculated using two methods: one based on the basic density of wood and the other based on the MC. The error between the MC calculated from wood density and that calculated from the MC was less than 10%, as reported by Batjargal *et al.* (2023).

The analysis of disks collected from different positions along the log length (0.2, 1.9, and 3.6 m from the stump) revealed that the IMC increased progressively towards the upper section of the log, while basic density exhibited the opposite trend (Fig. 5). This pattern can be attributed to variations in wood formation along the tree's length. The higher IMC in the upper portions is likely due to a greater proportion of juvenile wood, which is characterized by large cell lumens and thinner cell walls. In contrast, the lower sections contain a higher proportion of mature wood, which exhibits greater density due to thicker cell walls and higher lignification. The less pronounced variation in basic density compared to IMC suggests that additional factors, such as growth rate and wood extraction, may influence density along the log.

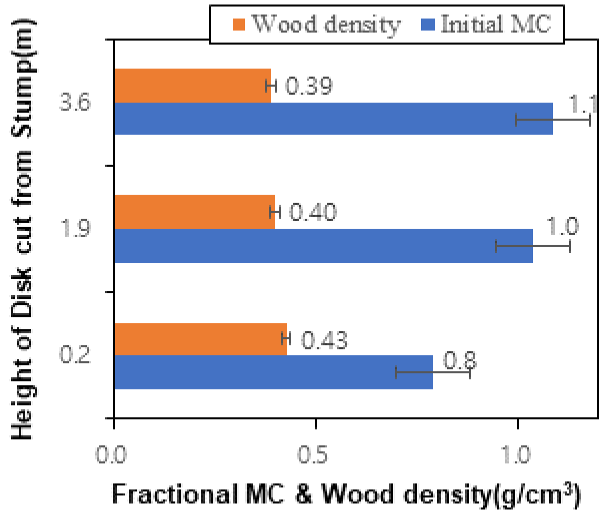

Fig. 5. IMC and basic wood density of timber

Average Moisture Content Changes during Drying

The average MC of the wood during drying was calculated based on the measured weight of the timber and the estimated oven dry weight. This was used to construct a drying curve that incorporated the actual drying conditions (temperature and humidity) and equilibrium moisture content (EMC), as illustrated in Fig. 6.

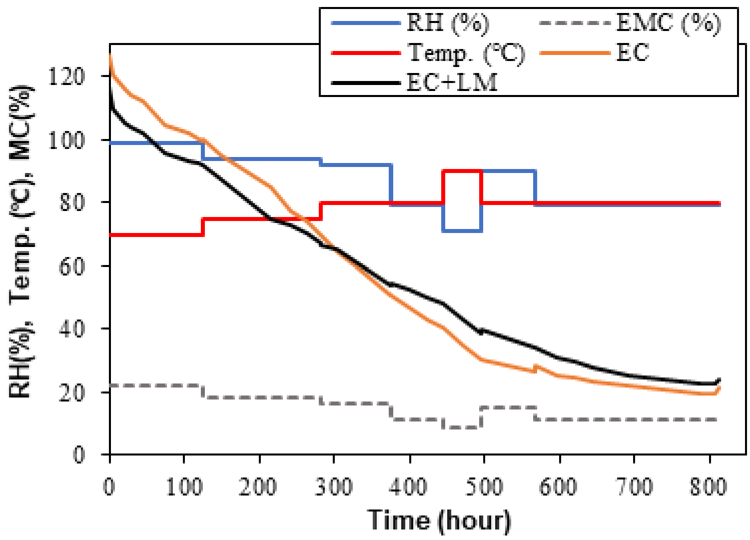

Fig. 6. Average MC of the two specimens and air temperature and humidity during kiln drying

The drying process was controlled to minimize defects by balancing the rate of moisture evaporation from the surface and movement from the interior of the wood. To maintain this balance, lateral moisturization was applied to the End Coating with Lateral Moisturization (EC + LM) test specimens after 300 h of drying. The drying process was completed after 800 hours, followed by a slow release of steam to gradually cool the wood. According to a previous study by Batjargal *et al.* (2023), in experiments involving the same wood species and similar heat drying conditions, the total drying time was 1200 hours. This difference in drying time could be attributed to variations in experimental conditions, such as temperature, humidity, and the specific characteristics of the wood.

Real-time Monitoring of MC changes in Timber during drying

The moisture content of the wood was indirectly estimated by calculating the EMC, considering the variations in relative humidity and temperature. The real-time monitoring results are shown in Fig. 7. The humidity was measured using a temperature and humidity sensor embedded in the wood. A comparison with the moisture content obtained from the Hailwood-Horrobin model revealed that the error between the estimated and measured MC was within 10%. However, due to the high moisture content during the early drying stages, the embedded temperature and humidity sensors frequently malfunctioned. To address this, the sensors were reinstalled after 300 hours of drying, as the initial readings were unreliable. As a result, no sensor data were available for the first 300 hours. To fill in the gap, estimated trend lines were constructed for temperature, humidity, and moisture content using the initial wood moisture content and actual drying chamber data.

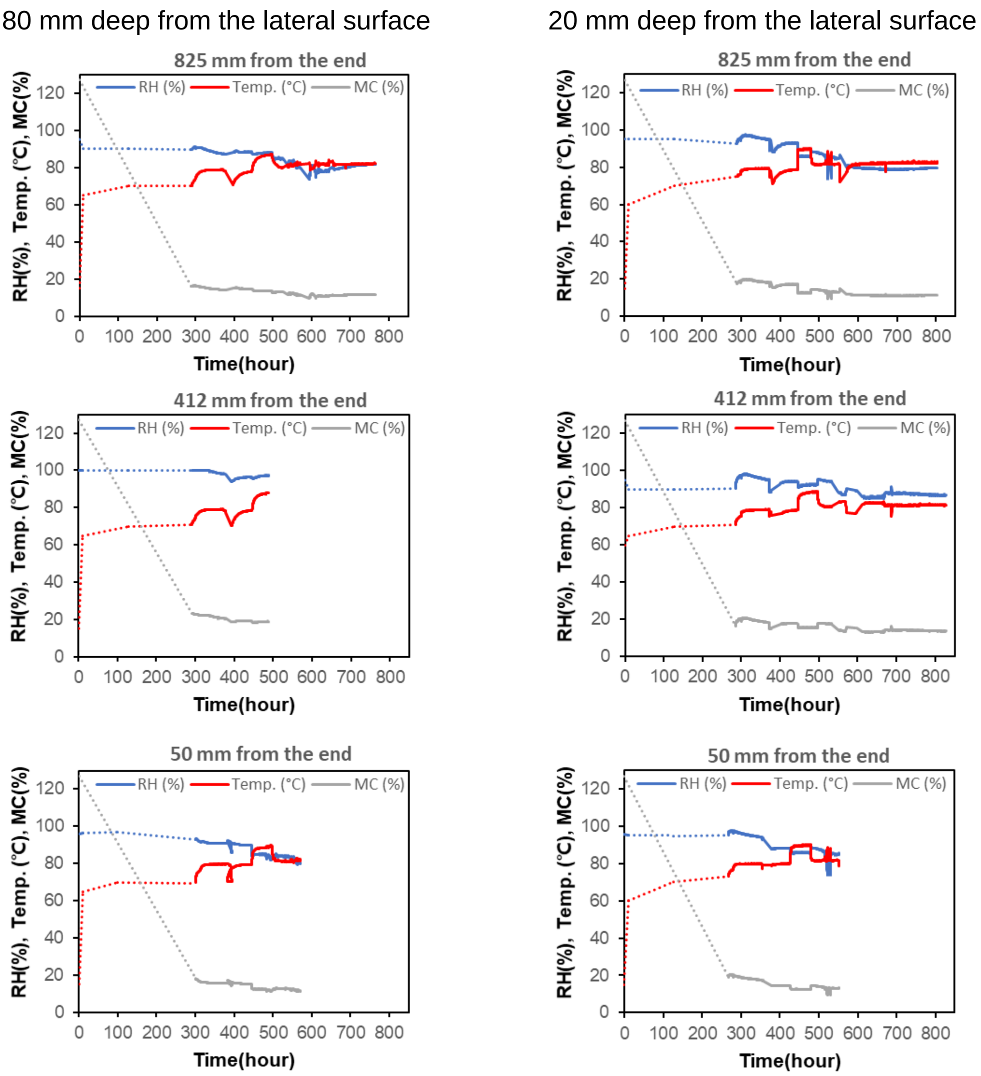

EC

EC+LM

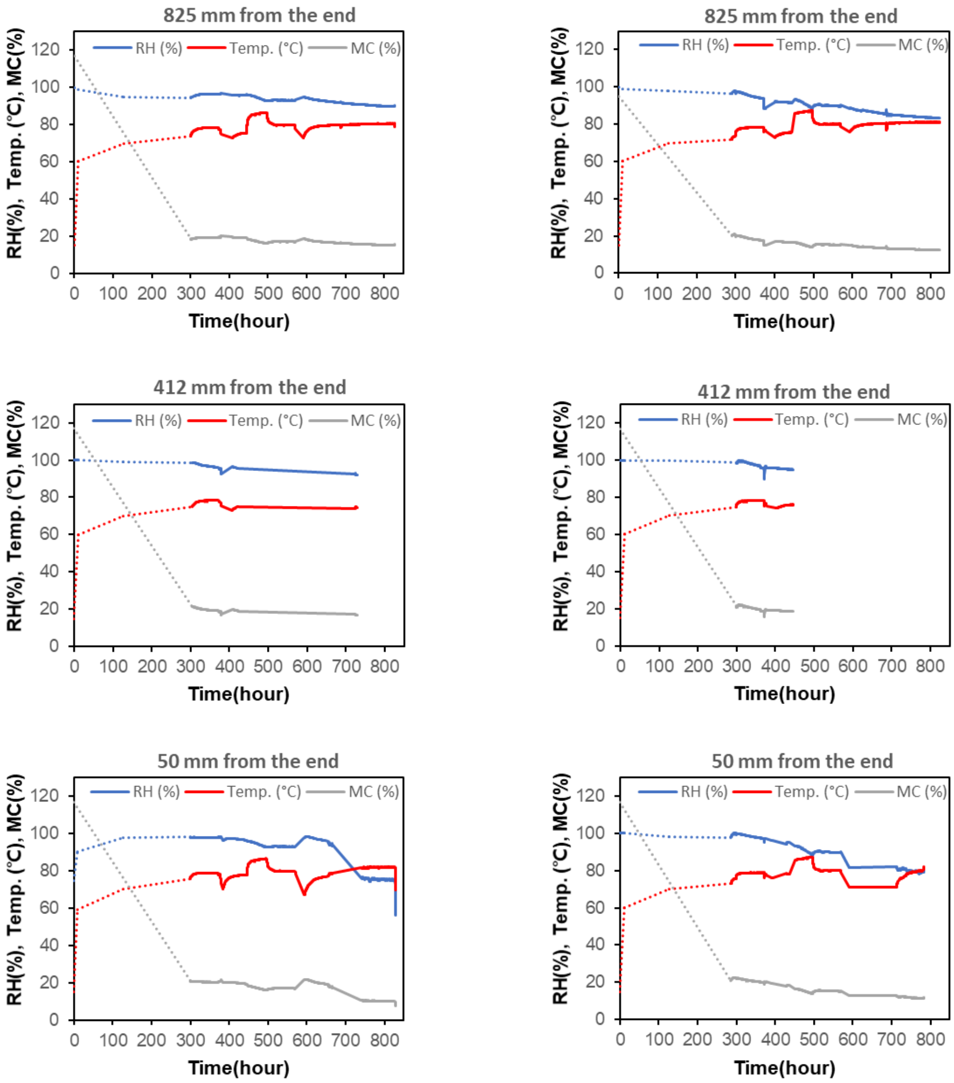

Fig. 7. Results of temperature and MC estimated from measured with temperature and humidity logger, EC: End Coating; EC+LM: End Coating + Lateral Moisturization

Final Moisture Profile

After drying, the MC distribution inside each specimen was analyzed, as shown in Fig. 8. the Average final MC of 20.7% (Fig. 8 (a)). In contrast, the average MC increased to 21.9% for the specimens treated with surface moisturization (EC+LM), with the surface MC measured at approximately 20%. This treatment contributed to a slight reduction in the moisture gradient compared to the untreated specimens. However, the potential influence of Step 5 (re-humidification) cannot be entirely ruled out, as it may have played a role in redistributing moisture within the wood. Further investigation is required to isolate the specific effects of re-humidification from those of the initial pretreatment. Additionally, the average MC in the 50 mm section of the cross-section was found to be 15%, indicating that moisture movement along the fiber direction was not completely inhibited, even when the ends of the specimen were coated with urethane waterproof paint. Observations in the drying chamber revealed that moisture evaporated rapidly from both ends of the specimen, resulting in the formation of split cracks at the cross-section. This process was documented through photographs taken throughout the drying period for further analysis.

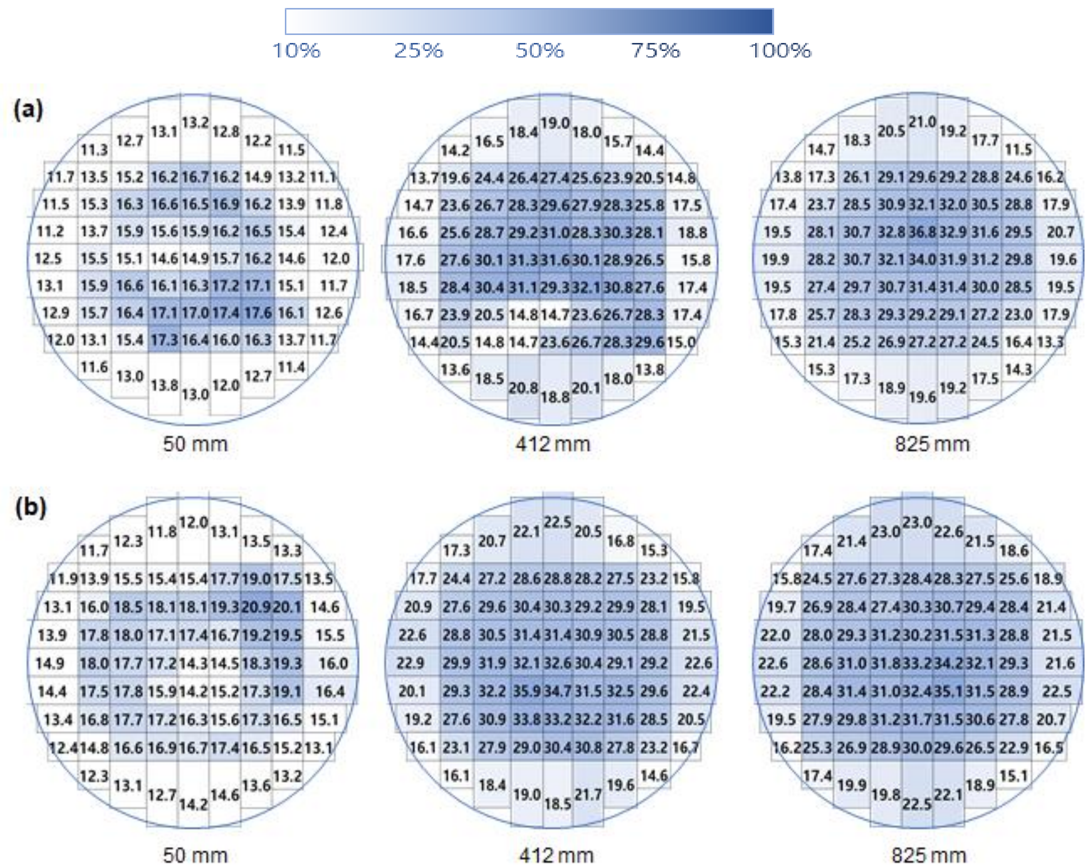

Fig. 8. Determine the final moisture profile: (a) End Coating, (b) End Coating with lateral Moisturization

Surface Checks Post Drying

The occurrence of surface checks after drying is summarized in Fig. 9. The total number of surface checks in EC+LM specimens was significantly lower than in EC specimens. The average moisture content at 412 mm and 865 mm was 23.8% for EC and 25.8% for EC+LM. The surface check investigation was conducted based on these moisture content levels.

The reduction in surface checks in EC+LM specimens suggests that the applied treatment effectively mitigated drying stresses, contributing to improved surface integrity. Specifically, the average area of the surface checks was 273.9 cm² per piece for the EC timber and 25.9 per piece for the EC+LM timber. These results suggest that the surface moisturization method effectively reduced the MC gradient within the timber, thereby minimizing drying defects.

Although the widths of the surface checks were similar for both wood types, lateral moisturization significantly reduced the number of checks. The observed reduction in surface checks can be attributed to the use of silica covers, which increased the EMC at the wood surface and reduced the moisture gradient-induced stresses during drying.

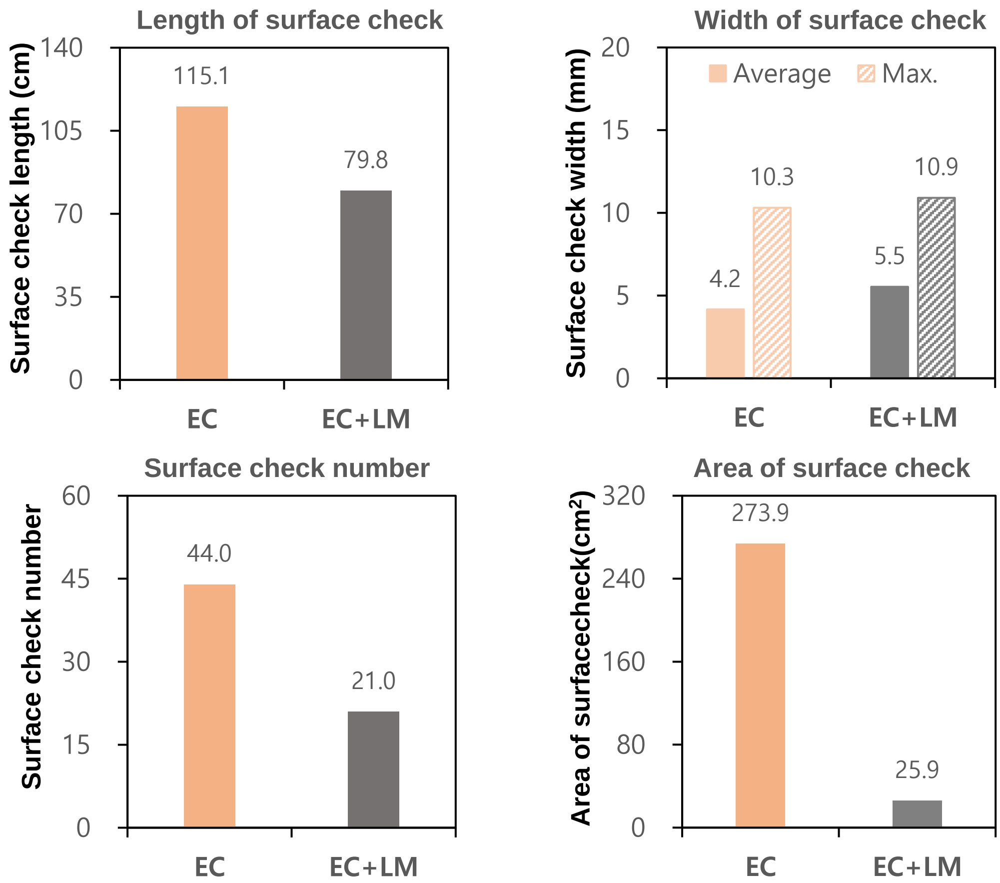

Fig. 9. Measurement of the dimensional occurrence of surface checks

Shrinkage Post-drying

The experimental results in Table 2 confirm that the shrinkage rate varied depending on the final moisture content after drying. The moisture contents of EC and EC+LM were 20.7% and 21.9%, respectively, indicating minimal differences. However, the shrinkage rates of the EC+LM and EC specimens were 0.5% and 0.8%, respectively. This suggests that lateral moisturization treatment effectively reduced shrinkage, likely by promoting a more uniform moisture distribution during drying.

Table 2. Transverse Shrinkage after Drying

Position from the butt of the log (mm)	EC (%)	EC+LM (%)
50	1.2	0.9
412	0.7	0.3
825	0.5	0.3
1238	0.6	0.3
1600	0.9	0.7
Average	0.8	0.5

CONCLUSIONS

This study experimentally investigated the effects of pretreatment methods, including end coating and lateral moisturization, on minimizing drying defects during kiln drying. The following conclusions are drawn from the test results:

1. Pretreating wood by coating the cross-sections to restrict moisture movement

along the grain direction while allowing moisture to evaporate solely in the transverse direction was not entirely effective in preventing surface checking.

2. Applying a lateral moisturizing treatment, which allows for gradual evaporation and reduces the moisture gradient, resulted in a slower drying process but effectively reduced surface checking. The controlled lateral moisturizing method introduced in the drying process of large-cross-sectional timber showed promising results in minimizing structural defects. This approach effectively mitigated the moisture gradient, a significant cause of drying-related issues such as checking and warping.

These findings provide valuable insights into how surface moisture control can mitigate wood-drying defects and enhance drying efficiency. Implementing these strategies can improve timber utilization. Furthermore, improving drying techniques plays a crucial role in preserving wooden cultural heritage sites and enhancing the structural integrity of timber for various construction applications, ultimately supporting the sustainable use of timber resources.

ACKNOWLEDGMENT

This research was supported by the Cultural Heritage Smart Preservation and Utilization R&D Program of the Cultural Heritage Administration, National Research Institute of Cultural Heritage (Project No. RS-2021-NC100101).

REFERENCES

Batjargal, B. U., Lee, T., Cho, M., Lee, C. J., and Yeo, H. (2023). "Effects of pretreatment for controlling internal water transport direction on moisture content profile and drying defects in large-cross-section red pine round timber during kiln drying," *Journal of the Korean Wood Science and Technology* 51(6), 493-508. DOI: 10.5658/WOOD.2023.51.6.493

Botter-kuisch, H. P., Van den bulcke, J., Baetens, J. M., and Van Acker, J., (2020). "Cracking the code: real-time monitoring of wood drying and the occurrence of cracks," *Wood Science and Technology* 54(4), 1029-1049. DOI: 10.1007/s00226-020-01200-6

Elustondo, D., Matan, N., Langrish, T., and Pang, S. (2023). "Advances in wood drying research and development," *Drying Technology* 41(6), 890-914. DOI: 10.1080/07373937.2023.2205530

Fu, Z., Zhao, J., Lv, Y., Huan, S., Cai, Y. (2016). "Stress characteristics and stress reversal mechanism of white birch (*Betula platyphylla*) disks under different drying conditions," *Maderas Cienc. Tecnol.* 18, 361-372.

Fu, Z., Chen, J., Zhang, Y., Xie, F., and Lu, Y. (2023). "Review on wood deformation and cracking during moisture loss," *Polymers* 15(15), article 3295. DOI: 10.3390/polym15153295

Green, D. W., Winandy, J. E., and Kretschmann, D. E. (1999). "Mechanical properties of wood," in: *Wood Handbook: Wood as an Engineering Material*, Madison, WI: USDA Forest Service, Forest Products Laboratory.

Han, Y., Chang, Y. S., Eom, C. D., and Lee, S. M. (2019a). "Moisture content change of Korean red pine logs during air drying: II. Prediction of moisture content change of Korean red pine logs under different air drying conditions," *Journal of the Korean Wood Science and Technology* 47(6), 732-750. DOI: 10.5658/WOOD.2019.47.6.732

Han, Y., Eom, C. D., Lee, S. M., and Park, Y. (2019b). "Moisture content change of Korean red pine logs during air drying: I. Effective air drying days in major regions in Korea," *Journal of the Korean Wood Science and Technology* 47(6), 721-731. DOI: 10.5658/WOOD.2019.47.6.721

Hill, C. A. S., Ramsay, J., Laine, K., Rautkari, L., and Hughes, M. (2013). "Water vapour sorption behaviour of thermally modified wood," *International Wood Products Journal* 4(3), 191-196. DOI: 10.1179/2042645313Y.0000000040.

Jung, J. Y., Ha. S. Y., and Yang, J. K. (2022). "Effect of steam explosion condition on the improvement of physicochemical properties of pine chips for feed additives," *Journal of the Korean Wood Science and Technology* 50(1), 59-67. DOI: 10.5658/WOOD.2022.50.1.59

Keey, R. B., Langrish, T. A. G., and Walker, J. C. F. (2000). *Kiln-Drying of Lumber*, Springer, Berlin, 326.

Kim, J. H., Yang, S. M., Lee, H. J., Park, K. H., and Kang, S. G. (2020). "A study on the evaluation and improvement of permeability in radial and tangential section of domestic softwoods," *Journal of the Korean Wood Science and Technology* 48(6), 832-846. DOI: 10.5658/WOOD.2020.48.6.832

Kim, H., Han, Y., Park, Y., Yang, S. Y., Chung, H., Eom, C. D., Lee, H. M., and Yeo, H. (2017). "Finite difference evaluation of moisture profile in boxed-heart large-cross-section square timber of *Pinus densiflora* during high temperature drying," *Journal of the Korean Wood Science and Technology* 45(6), 762-771.

Kollmann, F. F. P., and Côté, W. A. (1968). *Principles of Wood Science and Technology I: Solid Wood*, Springer-Verlag

Larsen, F., and Ormarsson, S. (2014). "Experimental and finite element study of the effect of temperature and moisture on the tangential tensile strength and fracture behavior in timber logs," *Holzforschung.* 68, 133-140.

Lee, N. H., and Lee, C. J. (2023). "Effects of pre-steaming treatment on high-temperature and low-humidity drying characteristics of super-heavy timber with boxed-heart of Korean red pine and Douglas-fir," *Drying Technology* 41(5), 794-803. DOI: 10.1080/07373937.2022.2119246

Lee, C. J. (2020). "Effect of kerfing and incising pretreatments on high-temperature drying characteristics of cedar and larch boxed-heart timbers with less than 150 mm in cross section size," *Journal of the Korean Wood Science and Technology* 48(3), 345-363. DOI: 10.5658/WOOD.2020.48.3.345

Li, C., Kang, C. W., and Zhao, X. F. (2019). "Moisture transverse moving mechanism during pre-steamed oak lumber drying," *Scientific Reports* 9(18228). DOI: 10.1038/s41598-019-54430-5

Oltean, L., Teischinger, A., and Hansmann, C. (2007). "Influence of temperature on cracking and mechanical properties of wood during wood drying—A review," *BioResources* 2(4), 789-811.

Park, Y., Chung, H., Kim, H., and Yeo, H. (2020). "Applicability of continuous process using saturated and superheated steam for boxed heart square timber drying," *Journal of the Korean Wood Science and Technology* 48(2), 121-135. DOI:10.5658/WOOD.2020.48.2.121

Penvern, H., Zhou, M., Maillet, B., Courtier-Murias, D., Scheel, M., Perrin, J., Weitkamp, T., Bardet, S., Caré, S., and Coussot, P. (2020). "How bound water regulates wood drying," *Physical Review Applied* 14(5), article 054051. DOI: 10.1103/PhysRevApplied.14.054051

Ra, J. (2014). "Determination of equilibrium moisture content of outdoor woods by using Hailwood-Horrobin equation in Korea," *Journal of the Korean Wood Science and Technology* 42(6), 653-658. DOI:10.5658/WOOD.2014.42.6.653

Redman, A. L., Bailleres, H., Turner, I., and Perré, P. (2016). "Characterisation of wood–water relationships and transverse anatomy and their relationship to drying degrade," *Wood Science and Technology* 50(4), 739-757. DOI: 10.1007/s00226-016-0818-0

Srisuchart, K., Tomad, J., Leelatanon, S., Jantawee, S., and Matan, N. (2023). "Internal stress development within wood during drying: A master curve concept and its application on drying stress evaluation," *Drying Technology* 41(15), 2516–2532. DOI:

10.1080/07373937.2023.2259467
Siau, J. F. (1995). *Wood: Influence of Moisture on Physical Properties*, Department of Wood Science and Forest Products, Virginia Polytechnic Institute and State University.
Simpson, W. T. (1991). *Dry Kiln Operator's Manual*. USDA Forest Service, Forest Products Laboratory, Agriculture Handbook, 188.
Simpson, W. T. (1973). "Predicting equilibrium moisture content of wood by mathematical models," *Wood and Fiber* 5(1), 41-49.
Skaar, C. (1988). "Hygroexpansion in wood," in: *Wood-Water Relations*, Springer Series in Wood Science, Springer, Berlin, Heidelberg. DOI: 10.1007/978-3-642-73683-4_4
Uwizeyimana, P., Perrin, M., and Eyma, F. (2020). "Moisture monitoring in glulam timber structures with embedded resistive sensors: study of influence parameters," *Wood Science and Technology* 54(6), 1463-1478. DOI: 10.1007/s00226-020-01228-8
Yin, Q., and Liu, H. (2021). "Drying stress and strain of wood: A review," *Applied Sciences* 11(11), article 5023. DOI: 10.3390/app11115023

Article submitted: January 10, 2025; Peer review completed: February 13, 2025; Revised version received: February 28, 2025; Accepted: April 8, 2025; Published: May 1, 2025.
DOI: 10.15376/biores.20.2.4761-4775